

KINETICS OF REACTION BETWEEN Mu AND Ni^{2+} IN SUPERHEATED WATER

G. Legate¹, C. Alcorn¹, J.-C. Brodovitch², K. Ghandi*¹, P.W. Percival*^{2,3},

¹Mount Allison University, Sackville, New Brunswick, Canada

²Simon Fraser University, Burnaby, British Columbia, Canada

³TRIUMF, Vancouver, British Columbia, Canada

Abstract

Rates of spin exchange of muonium with Ni^{2+} in sub and supercritical D_2O were investigated using muon spin spectroscopy (μSR). The procedure for determining rate constants of muonium reactions is described. Then, results for the reaction of muonium with Ni^{2+} in D_2O are compared to previous data obtained for Ni^{2+} in H_2O . The rate constants are presented as functions of temperature, pressure, viscosity and density to explore possible contributions to the solvent isotope effects.

1. Introduction

The work described in this paper furthers current knowledge of water chemistry under the extreme conditions that will be present in a future generation of pressurized-water-cooled nuclear reactors.

In this work, the rates of spin exchange of muonium with Ni^{2+} in heavy water above and below the critical point were investigated using muon spin spectroscopy (μSR). Muonium ($\text{Mu} = \mu^+ e^-$) is considered to be a light isotope of hydrogen and has a rest mass 1/9 the mass of atomic hydrogen [1, 2]. A spin-exchange reaction is one in which there is no observable atomic rearrangement of reactants; instead, reactants having one or more unpaired electrons interact to effect a mutual change of electron spin orientation. Since barriers for spin exchange are usually very small, a spin exchange “reaction” is an ideal system to study the effects of transport and “solvent cage” on the kinetics of chemical reactions without worrying about solvent effects on activation barriers [3]. Results obtained from this work are also relevant to other reactions possessing low activation-energy barriers. Two other presentations in this conference deal with activation-controlled reactions of Mu .

μSR was chosen because it avoids the disadvantages of conventional pulsed radiolysis, which employs optical spectroscopy or electron spin resonance (ESR) detection methods to determine rate constants of the H atom and other reactive intermediates from the radiolysis of water [3]. The basis of the μSR technique is single-event counting, and with only one Mu atom in the system at a time Mu decay kinetics is always pseudo-first order. Secondary reactions resulting from complex mechanisms will not affect the observed kinetics because the products of the primary Mu reaction are effectively invisible (spin dephased). Similarly, wall reactions can be ignored, since at the densities of interest the diffusion time of Mu atoms to the walls of the target vessel is typically much longer than the muon lifetime. Thus the μSR technique is immune to many of the systematic errors and complications of H-atom

kinetics studies. Also, our μ SR experiments use a beam of high energy positive muons (μ^+) that can penetrate the windows of high pressure vessels. Most of the decay positrons (see experimental section) also have enough energy to pass through the thick walls of the high pressure vessel. Therefore, using μ SR allows us to study reactions under conditions which resemble as much as possible those of a Generation IV Supercritical-Water-Cooled Reactor (SCWR).

When the beam of positive muons enters the pressure vessel (sample cell), the muons can capture electrons from the end of the radiation track to form Mu, which then reacts with the solute. In the work described here, the Mu electron (spin polarized) undergoes spin exchange with a nickel electron (not polarized), and the rate constant is obtained from the decay (spin depolarization) of the Mu signal [1-3]. The reaction was investigated under a variety of conditions, and the rate constants determined for H₂O and D₂O solvents were inspected as functions of temperature, pressure, viscosity and density to explore possible contributions to the solvent isotope effects.

2. Experimental

The μ SR experiments were carried out at TRIUMF in Vancouver, BC, Canada, using the M9B muon beam-line. Muons are generated by bombarding a target with high energy protons. This results in the generation of positive pions that decay into muons and neutrinos ($\pi^+ \rightarrow \mu^+ + \nu_\mu$) [1, 2]. Since spin angular momentum must be conserved, the decay of spin-zero pions generates muons and neutrinos with opposite spin. Similarly, consideration of helicity and the conservation of linear momentum requires that each muon has spin and linear momentum in opposite directions. By judicious selection of momentum it is possible to tune the beam line for a high degree of muon spin polarization (> 80%).

As each muon approaches the sample cell it triggers an electronic clock and then comes to rest in the sample, where it decays. The clock is stopped when the muon decay positron is detected. A histogram is generated from the number of muon-positron correlated events against elapsed time. When a magnetic field is applied transverse to the muon spin polarization, the muon lifetime decay curve for each positron detector is modulated by the probability of positron detection in that direction. This is because the muon spins precess in a transverse magnetic field, and the probability of positron detection has an angular dependence, with the maximum along the spin direction at the time of decay. The resulting μ SR histogram has the general form [1, 2]

$$N(t) = N_0 e^{-t/\tau_\mu} [1 + A(t)] + b \quad (1)$$

where N_0 is an overall normalization factor which depends on the number of stopped muons and the detector geometry, b represents random accidental (background) events, $\tau_\mu = 2.197 \mu\text{s}$ is the muon lifetime, and $A(t)$ represents the “asymmetry”, which describes the μ SR signal of interest. For transverse field μ SR the muon asymmetry is analogous to the free induction decay signal of conventional pulsed magnetic resonance spectroscopy.

The asymmetry includes contributions from all muon environments, i.e. paramagnetic Mu and diamagnetic species such as MuH and MuOH. The components of the signal in a transverse

magnetic field (TF) can each have different precession frequencies (ω_i), phases (ϕ_i), amplitudes (A_i) and relaxation rates (λ_i), so in general

$$A(t) = \sum_i A_i \exp(-\lambda_i t) \cos(\omega_i t + \phi_i). \quad (2)$$

The precession frequencies of muon spins in different diamagnetic environments are indistinguishable — they all precess practically at the muon Larmor frequency. The muonium signal is characterized by much faster precession. At low TF (5 G was used in this study) the μ SR signal has only two components:

$$S(t) = A_{\text{Mu}} e^{-\lambda_{\text{Mu}} t} \cos(\omega_{\text{Mu}} t + \phi_{\text{Mu}}) + A_{\text{D}} e^{-\lambda_{\text{D}} t} \cos(\omega_{\text{D}} t + \phi_{\text{D}}) \quad (3)$$

The “triplet” Mu precession frequency ω_{Mu} is 103 times faster than the diamagnetic muon precession frequency, ω_{D} . At higher (> 20 G) fields ω_{Mu} splits into two frequencies.

The relaxation of the Mu signal (λ_{Mu}) is of particular importance since it represents chemical decay of muonium and/or spin relaxation caused by interaction of Mu with other paramagnetic atoms or molecules. In general, the diamagnetic muon relaxation rate is slow enough to be ignored in studies of Mu reactivity in liquids.

In the homogeneous kinetics regime of interest in this work, the time dependence of the muon polarization in the Mu atom can be represented by the simple first-order decay expression:

$$[\text{Mu}]_t = [\text{Mu}]_0 e^{-\lambda t} \quad (4)$$

where $\lambda = k_{\text{Mu}}[\text{X}]$ is a pseudo first-order rate constant and k_{Mu} is the second-order rate constant for the reaction of Mu with reactant “X”.

There is also a background relaxation, λ_0 , due to muonium reaction with the solvent and/or due to physical/instrumental effects. To account for this, data was obtained for Mu relaxation in the pure solvent over a wide range of conditions. A polynomial fit of these data as a function of density was then used to determine λ_0 under the appropriate thermodynamic conditions. The rate constant for reaction is then obtained from the expression: $\lambda = \lambda_{\text{Mu}} - \lambda_0$. Muon decay rates can then be converted to rate constants using the following equation.

$$k_{\text{Mu}} = \frac{\lambda_{\text{Mu}} - \lambda_0}{[\text{X}]} \frac{\rho_0}{\rho(T, P)} \quad (5)$$

where k_{Mu} is the rate constant, λ_{Mu} is the total muonium relaxation rate measured in the experiment, λ_0 is the background relaxation, $[\text{X}]$ is the concentration of the reactant present in solution, ρ_0 is the density at standard temperature and pressure, and $\rho(T, P)$ is the density at the temperature and pressure of the measurement.

The spin exchange of Ni^{2+} with muonium was studied over a range of temperatures, from 25°C to 385°C, and for pressures from 1 bar to 350 bar. Samples of nickel chloride dissolved in deuterium (D_2O) were prepared at approximately 50 μM and 100 μM concentrations, and

deoxygenated by cycles of pumping and bubbling of argon gas. The prepared samples were then transferred into a high pressure cell which is made of titanium alloy (Ti6Al-4V) and safety rated to sustain pressures of up to 500 bar at 500°C.

Our sample handling consists of a network of stainless-steel capillary tubes, valves and T-tube fittings (Figure 1).

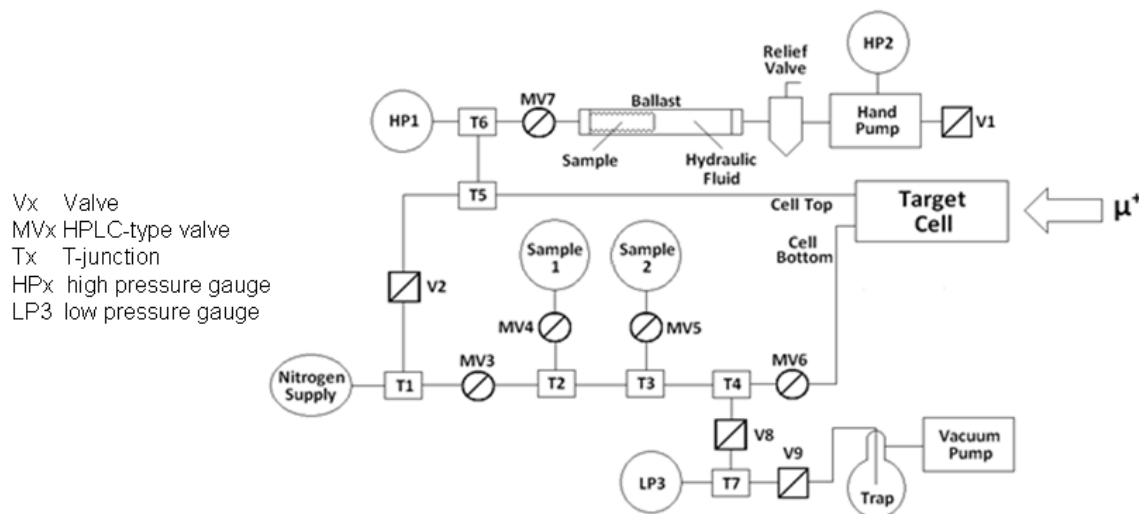


Figure 1. Schematic of experimental setup. Valves 8 and 9 are low pressure valves, whereas all others are rated for high pressure.

Samples are connected to the system through Swagelok to glass fittings, valved off with HPLC-valves MV4 and MV5. For sample transfer, the cell is first evacuated, then transfer to the cold target cell (volume ~ 30 mL) is effected by opening the sample valve and MV6, whereupon the sample liquid stored in the pressurized sample bulb (~2 bar of argon gas) flows into the evacuated cell. Samples are removed from the cooled target cell at the conclusion of a series of measurements by applying vacuum at the bottom of the target cell while applying a pressure of nitrogen gas to the top.

During experiments valves V2 and MV6 are closed, but MV7 is open. This allows the sample to expand from the heated target cell into the ballast volume, where a thin, stainless-steel bellows arrangement separates the aqueous sample from a hydraulic fluid, whose purpose is to allow for independent pressure control via the hand pump. A pressure relief valve is set to limit the pressure to a safe value (typically 350 bar). The temperature is regulated with a standard PID controller that controls a commercial heating element (Watlow) wrapped non-inductively around the body of our target cell.

Experiments were carried out with the muon beam-line momentum set to 75 MeV/c, except for samples of very low density (~0.1 g cm⁻³), when momentum was reduced to 70 MeV/c. The purpose is to ensure that the incoming muons penetrate the cell window but then stop in the sample.

D₂O (Cambridge Isotope Laboratories, Inc. 99.9% D) was used without further purification. To minimize possible cross contamination, samples were studied in order of increasing concentration.

3. Results and discussion

This section presents the results of experiments performed at TRIUMF in June 2009 (Table 1), and compares the data with earlier results obtained in H₂O solutions [3].

Temperature (°C)	Pressure (bar)	Density (g cm ⁻³)	Viscosity (cP)	k_{Mu} (10 ¹⁰ M ⁻¹ s ⁻¹)
20	233	1.117	1.223	2.6 ± 0.3
25	232	1.116	1.070	2.3 ± 0.5
30	233	1.115	0.980	2.9 ± 0.5
50	230	1.107	0.652	3.9 ± 0.5
60	231	1.102	0.560	2.2 ± 0.6
80	232	1.089	0.420	6 ± 1.3
130	233	1.050	0.254	7 ± 1.5
180	231	0.999	0.176	12 ± 3
230	230	0.936	0.135	11 ± 3
280	231	0.856	0.109	10 ± 1.6
330	233	0.744	0.087	11 ± 1.5
340	233	0.713	0.083	13 ± 2
360	230	0.625	0.070	9 ± 2
365	231	0.594	0.065	15 ± 2
375	230	0.414	0.042	4.7 ± 0.4
375	240	0.504	0.054	10 ± 0.6
375	250	0.537	0.059	10 ± 1
375	234	0.468	0.049	10 ± 1.3
385	230	0.186	0.028	3.8 ± 0.5
385	302	0.546	0.061	15 ± 1.5
385	240	0.226	0.030	4.9 ± 0.3
385	250	0.300	0.035	5.2 ± 0.4
385	260	0.400	0.044	8.0 ± 0.4
385	269	0.458	0.050	10 ± 0.6
385	277	0.490	0.094	12 ± 0.7
385	287	0.517	0.057	10 ± 0.9
385	301	0.577	0.061	11 ± 0.9
385	312	0.560	0.063	12 ± 1.5
385	323	0.573	0.064	12 ± 1.3
385	343	0.593	0.067	11 ± 1.4
385	258	0.382	0.042	6.1 ± 0.5
385	230	0.189	0.028	6 ± 3

Table 1: Data obtained at TRIUMF in June 2009 for the reaction of Mu with Ni²⁺ in D₂O

The data for D₂O was obtained at pH 5.5 but the data for H₂O was obtained at pH 4.5. The pH of the system might be important since the speciation (dissociation) of NiCl₂ is pH dependent [4]. For the pH values of the current work, NiCl₂ is 100% dissociated at low temperatures in water [4]. However there is no equivalent published data for the high-temperature range of our studies in D₂O.

The rate constant was found to increase with temperature up to approximately 330°C (at ~250 bar) in both H₂O and D₂O. After this point, the rate constant reaches a plateau, followed by a subsequent decrease. This finding has been rationalized as being due to a cage effect, i.e. the interaction of solvent molecules about two reactant molecules keeps them together so that there are many collisions between the reactants per encounter, thereby increasing the probability of spin exchange [3]. Such cage effects do not exist in the gas phase and the decrease of encounter time at higher temperatures as the liquid approaches supercritical conditions causes an inefficient spin exchange; hence the rate constant decreases at high temperatures. It should be emphasized that close to the critical point the fluid differs from the liquid and gas phases due to its density inhomogeneity.

The encounter time can be estimated using equation 6 where k_{diff} is the diffusion-limited rate constant and $[\text{H}_2\text{O}]$ is the concentration of H₂O (or D₂O) [3].

$$\tau_{\text{enc}} = \frac{8k_{\text{diff}}^{-1}}{[\text{H}_2\text{O}]} \quad (6)$$

At elevated temperatures and low densities, the number of collisions per encounter falls, and therefore the probability of reaction decreases under supercritical conditions [3].

Until recent work [3, 5-7], estimates of the kinetics of transient species involved in the radiolysis of water under the extreme conditions of a SCWR were based on extrapolations from data obtained at much lower temperatures [8] using either diffusion-limited rate constants (equation 7) or the Noyes equation (equation 8).

For diffusion-limited reactions, the Smoluchowski equation (7) is widely used [8]:

$$k_{\text{diff}} = 4000\pi(D_A + D_B)r_{\text{AB}} N_{\text{Av}} \quad (7)$$

where k_{diff} is the diffusion-controlled rate constant, D_A and D_B are the diffusion coefficients of the reactants, r_{AB} is the distance at which reactants A and B can react and N_{Av} is the Avogadro number (6.022×10^{23}).

The kinetics of reactions that are close to the diffusion limit, and are therefore subject to both diffusion and activation processes, can be modelled by the Noyes equation:

$$1/k_{\text{obs}} = 1/k_{\text{diff}} + 1/k_{\text{react}} \quad (8)$$

where k_{obs} is the observed rate constant and k_{react} is the activation-controlled rate constant:

$$k_{\text{react}} = Ae^{-E_a/k_B T} \quad (9)$$

where E_a is the activation energy of the reaction, k_B is the Boltzmann constant, T is the temperature and A is a pre-exponential factor.

The diffusion coefficients in equation 7 are often calculated using equation 10:

$$D = \frac{k_B T}{n\pi\eta R_0} \quad (10)$$

where η is viscosity and R_0 is the hydrodynamic radius.

At the critical point, a large increase in kinetic mobility of reaction species has been noted, and the diffusion rates of water under supercritical conditions were found to be approximately 60 times larger than those determined under standard conditions [9].

In the strong-exchange limit the rate constant of spin-exchange processes depends only on the diffusion-limited rate constant and p_{spin} , the probability of a spin exchange (8/27 for Ni^{2+} and muonium at low field [10]). However, in the general case the probability depends on the encounter lifetime and the strength of the exchange interaction J [3].

$$k_{\text{ex}} = p_{\text{spin}} k_{\text{diff}} f_J; \quad f_J = J^2 \tau_{\text{enc}}^2 / (1 + J^2 \tau_{\text{enc}}^2). \quad (11)$$

The spin exchange factor f_J can be determined experimentally from the obtained rate constant, the diffusion-limited rate constant (k_{diff}) and p_{spin} .

The fact that our experimental rate constants go through a maximum just prior to the critical point shows that the strong exchange limit does not provide an adequate model for rate constants under extreme conditions.

Figure 2 displays our experimental rate constant data plotted as functions of various parameters (temperature, pressure, viscosity and density) to facilitate discussion of potential contributions to solvent isotope effects.

There are significant differences between the observed spin exchange rate constants in D_2O and H_2O . There could be three general reasons for these differences:

- 1) Our initial data on H_2O solutions [3] might be at fault. These were our very first measurements and done with a different pressure cell and ballast design. The cell was made from stainless steel, not the current material which is a passivated titanium alloy, and might have corroded under supercritical conditions, or otherwise influenced the Ni^{2+} concentrations. The previous ballast design was based on a piston that moved inside a cylinder, with hydraulic oil on one side and the sample on the other side. It could be possible that a small amount of oil leaked past the seal and contaminated the sample. This is not possible with the current design of bellows.
- 2) The D_2O used in this study could have had some unknown contamination that would react with Mu. In general, when repeating measurements under the same experimental conditions, the smaller rate constants are more believable since usually greater contamination would result in larger relaxation rates. Contamination from either distilled water or D_2O is less likely than contamination from our apparatus, since we used a few different concentrations of Ni^{2+} in both H_2O or D_2O . Measurements at different concentrations should eliminate the systematic errors due to impurities in the solvent, unless the impurities react with Ni^{2+} .

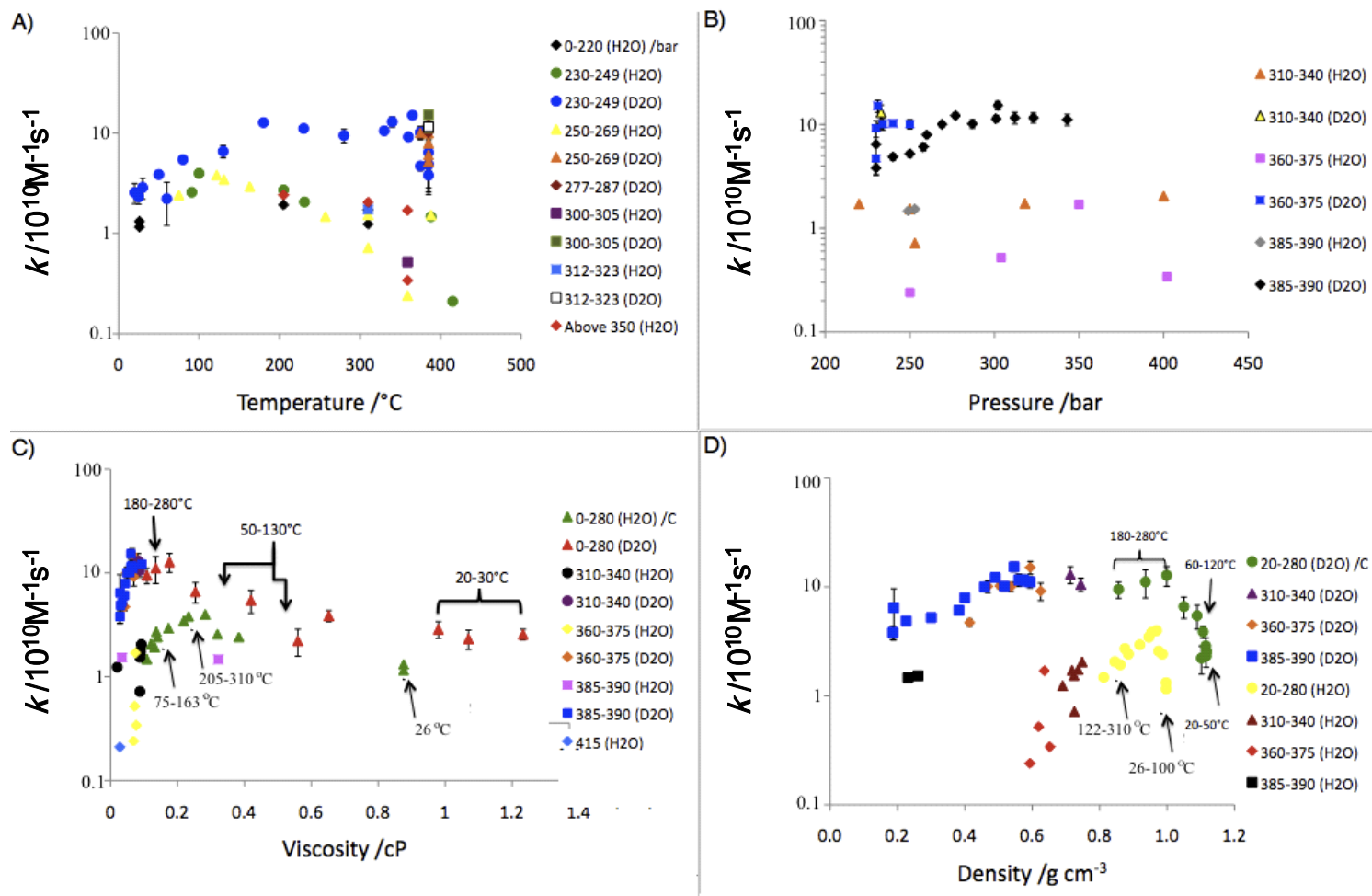


Figure 2: Rate constants for the reaction of muonium with Ni^{2+} in D_2O and in H_2O . The data is displayed as a function of: A) temperature (with points at different pressures); B) pressure (with points at different temperatures); C) viscosity (with points at different temperatures); and D) density (with points at different temperatures).

- 3) The differences in rate constants are due to solvent kinetic isotope effects, possibly caused by differential binding of H₂O and D₂O in the Ni²⁺ coordination shell.

Table 2 summarizes the solvent isotope effects (ratios of rate constants in D₂O vs. H₂O) for different density ranges. Figure 3 shows this data in the form of a plot. The maximum discrepancy (difference) between the rate constants in the two solvents is at intermediate densities.

Density Range (g cm ⁻³)	Average Density (g cm ⁻³)	Ratio of rate constants (D ₂ O/H ₂ O)
1.117 - 0.936	1.044	2 ± 3
0.857 - 0.856	0.859	4.32 ± 0.7
0.744 - 0.713	0.725	6.6 ± 1.4
0.625 - 0.690	0.658	7.4 ± 1.4
0.594 - 0.504	0.536	19 ± 4
0.468 - 0.414	0.436	5.8 ± 1.5
0.231 - 0.266	0.229	3.3 ± 0.2

Table 2: Solvent isotope effect for rate constants in D₂O and H₂O.

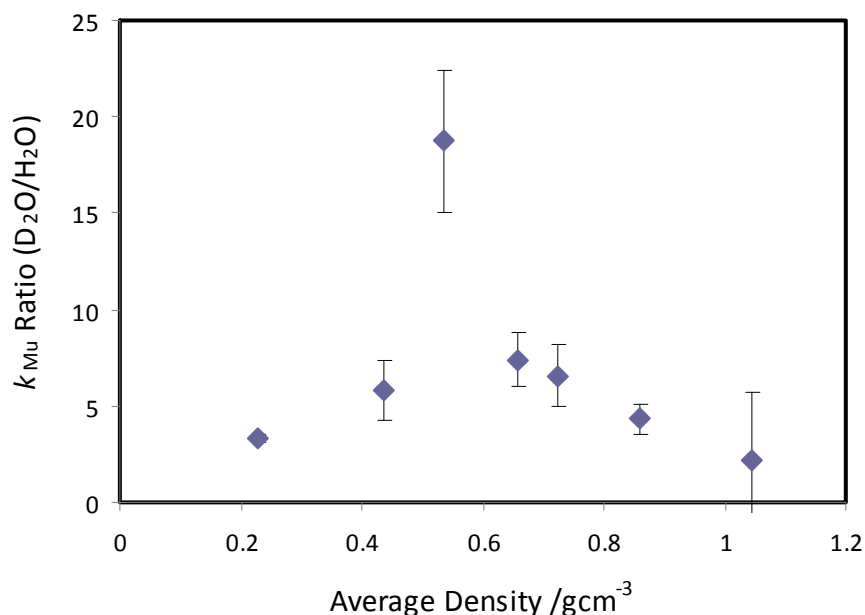


Figure 3: Solvent isotope effects between H₂O and D₂O at different densities.

Figure 2(A) shows the temperature dependence of the rate constant for Mu with Ni²⁺ in both D₂O and H₂O. In D₂O, the rate constant goes through a maximum before the critical point, over the approximate temperature range of 240-350°C. The difference in rate constants in the

two solvents is small at low temperatures and increases with temperature. Since higher temperatures are relevant for the GenIV SCWR design, it is recommended that these measurements be repeated in both solvents at a few different concentrations and at different magnetic fields (to distinguish spin exchange from other potential processes [10]). Discussion of the potential source of the isotope effects must wait for these future experimental results.

Figure 2(B) reveals only small pressure dependence of the rate constants, but for the high temperature data shown here the rate constants are close to an order of magnitude larger in D₂O than in H₂O.

Figure 4 is a comparison of the experimental data for D₂O with the diffusion-limited rate constant calculated by scaling the room temperature value by T/η . It is evident that the reaction rates reach the diffusion-limit over only a small range. At high densities the rate constant is consistent with a diffusion-limited process, which supports the view that the reaction studied is a spin-exchange process in the strong exchange limit.

Assuming that the rate constant determined for D₂O is due to spin exchange between Ni²⁺ and Mu, analysis according to equation 11 leads to a value of J of $1.0 \pm 0.4 \times 10^{12} \text{ rad s}^{-1}$ (Figure 5). The value obtained for H₂O solutions [3] is similar: $J = 1.4 \pm 0.2 \times 10^{12} \text{ rad s}^{-1}$. Since these results are reasonably consistent with expectations, it is possible that, despite the observation of significant differences for the two solvents, the measured rate constants correspond indeed to spin exchange reaction with Ni²⁺.

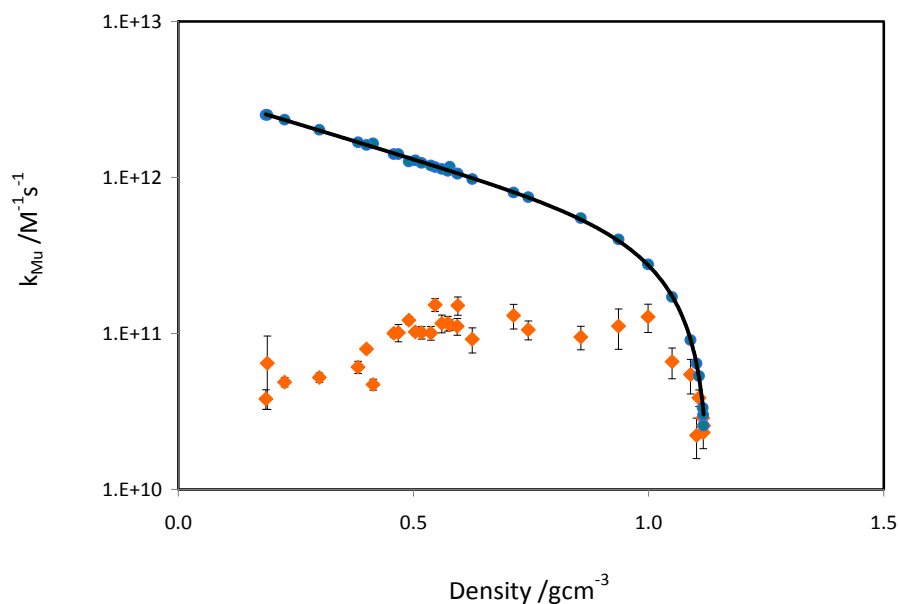


Figure 4: The diffusion-limited rate constant (blue circles) and the experimentally observed rate constant (orange diamonds) for Mu + Ni²⁺ in D₂O, plotted versus density.

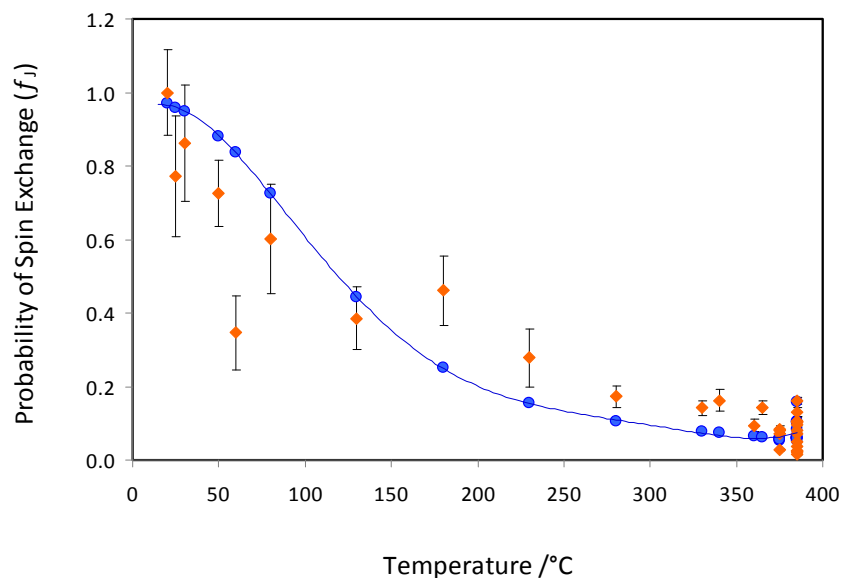


Figure 5: The theoretical spin exchange probability (blue circles) compared with values determined from the experimental data for $\text{Mu} + \text{Ni}^{2+}$ in D_2O . The blue curve through the theoretically calculated points at the same thermodynamics conditions of the experiments is to guide the eyes.

4. Conclusion

Measurements made at TRIUMF have been analysed to determine rate constants for the reaction of Mu with Ni^{2+} in D_2O . Comparison of the results with previous data for $\text{Mu} + \text{Ni}^{2+}$ in H_2O revealed large differences in rate constants for the two solvents under the same conditions. The apparent solvent isotope effects may be real or an artefact of errors in our measurements. A general observation for both sets of data is that the rate constants go through a maximum with temperature and then a plateau followed by a subsequent decrease. The rate constants can be modelled by assuming spin exchange between Mu and Ni^{2+} , but the reaction is only diffusion-limited over a small range of thermodynamic conditions (low temperatures and large densities).

Future work will include repetition of some measurements in both H_2O and D_2O .

5. Acknowledgments

We thank Dr. Syd Kreitzman and the staff of the TRIUMF μSR facility for their technical support. Financial support from the NSERC/NRCan/AECL Generation IV Energy Technologies Program is also greatly appreciated.

6. References

- [1] D. C. Walker, *J. Chem. Soc., Faraday Trans.*, 94, 1998, 1.
- [2] E. Roduner, *Prog. React. Kinet.*, 14, 1986, 1.
- [3] K. Ghandi, B. Addison-Jones, J. Brodovitch, I. Mackenzie, P. W. Percival and J. Schüth, *Phys. Chem. Chem. Phys.*, 4, 2002, 586.

- [4] J. Jinxing and C. Cooper, *Electrochimica Acta.*, 41, 9, 1996, 1549.
- [5] K. Ghandi and P. W. Percival, *J. Phys. Chem. A*, 107, 17, 2003, 3005.
- [6] K. Ghandi, B. Addison-Jones, J.-C. Brodovitch, S. Kecman, I. McKenzie, P. W. Percival, *Physica B*, 326, 2003, 76.
- [7] T. W. Marin, J. A. Cline, K. Takahashi, D. M. Bartels, C. D. Jonah, *J. Phys. Chem. A*, 106, 2002, 12270.
- [8] A. J. Elliot, D. R. McCracken, G. V. Buxton, N. D. Wood, *J. Chem. Soc. Faraday Trans.*, 86, 1990, 1539.
- [9] I. M. Svishchev and A. Plugatyr, *J. Supercritical Fluids*, 37, 2006, 94.
- [10] M. Senba, *Phys. Rev. A*, 52, 1995, 4599.